K14-Ang1 mice appeared normal, and histological sections revealed that the ear skin was similar to that of wild-type mice in terms of both thickness and cellular components; the only obvious difference in the K14-Ang1 skin was an increased number of large vessels. In contrast, the ear skin of K14-VEGF mice appeared thicker than normal (3), and by the time the mice were 10 to 12 weeks of age focal red skin lesions began to develop in their ears. We focused on the ear skin of mice because (i) the vasculature is not obscured by dense hair, (ii) the ear vasculature can easily be examined in whole mounts, (iii) the ears can easily be examined while the mice are alive, and (iv) the ear skin seemed to resemble the remainder of the skin. Different amounts of Ang1 or VEGF expression in different regions of skin, perhaps as a result of different density of hair follicles, could result in quantitative differences in vessel length and area density.

7. The phenotype of the ear microvessels was determined by examining the venule-specific endothelial cell markers P-selectin and von Willebrand factor (vWF) (*23*) and the pericyte marker desmin. In K14-Ang1 mice we found strong immunoreactivity for P-selectin and vWF in venules and in vessels in the anatomic position of capillaries, but in wild-type mice we found strong immunoreactivity for these markers only in venules. Further, the pericytes of these vessels in K14-Ang1 mice had the highly branched morphology of venules instead of the elongated morphology of capillaries.
8. The vessel length density in ear skin of K14-VEGF mice (63.5 ± 2.8 mm/mm^2) was 56% greater than that in wild-type mice (40.7 ± 1.2 mm/mm^2) and 37% greater than that in K14-Ang1 mice (46.3 ± 2.4 mm/mm^2). In contrast, the average capillary diameter in K14-Ang1 mice (15.8 ± 0.8 μm) was 90% greater than that in wild-type mice (8.3 ± 0.6 μm) and 147% greater than that in K14-VEGF mice (6.4 ± 0.3). The vessel length density in K14-Ang1/VEGF mice was further increased (66.7 ± 3.9 mm/mm^2), whereas the average capillary diameter was normal (8.7 ± 0.1 μm) due to averaging unusually large and small vessels. Supplementary material is available at www.sciencemag.org/feature/data/1043334.shl
9. H. Inoue *et al.*, *Eur. J. Pharmacol.* **333**, 231 (1997).
10. An inflammatory agent, mustard oil or serotonin, known to cause plasma leakage in mouse skin (*9*, *24*), was applied to the ear 1 min after injection of Evans blue dye. Mustard oil (Sigma) was diluted to 5% in mineral oil and applied to the dorsal and ventral surfaces of the ear with a cotton tip; it was reapplied 15 min later. Nothing was done to the other ear of mice treated with mustard oil (baseline control). Serotonin (Sigma) was dissolved at 0.22 mg/ml in sterile 0.9% NaCl plus 0.005 N acetic acid (vehicle). About 10 μl was injected (28G needle) intradermally into the dorsal ear skin, and a similar volume of vehicle was injected into the other ear (control). Thirty minutes after the stimulus, the vasculature was perfusion-fixed (1% paraformaldehyde in 50 mM citrate buffer, pH 3.5) for 2 min. Ears were removed, blotted dry, and weighed. Evans blue was extracted from the ears with 1 ml of formamide overnight at 55°C and measured spectrophotometrically at 610 nm.
11. E. Fujii *et al.*, *Naunyn-Schmiedebergs Arch. Pharmakol.* **350**, 361 (1994).
12. Injection of PAF (80 μg/ml) in the ear skin of wild-type mice increased Evans blue content to 41.2 ± 10.0 ng/mg, whereas in K14-Ang1 mice the amount was 23.2 ± 4.1 ng/mg (n = 3).
13. B. W. Zweifach, *Annu. Rev. Physiol.* **35**, 117 (1973).
14. Because ricin binds more avidly to components of the basement membrane (*25*) than to the endothelial cell surface, it can be used to identify the number and location of sites of exposed basement membrane (*26*). Perfusion of ricin after fixation helps to eliminate the role of blood flow and pressure.
15. G. Majno, G. E. Palade, G. I. Schoefl, *J. Biophys. Biochem. Cytol.* **11**, 607 (1961); E. Svensjo and G. J. Grega, *Fed. Proc.* **45**, 89 (1986); D. M. McDonald, *Am. J. Physiol.* **266**, L61 (1994).
16. We found fewer ricin-labeled leaky vessels in double transgenic K14-Ang1/VEGF mice than in K14-VEGF mice after treatment with mustard oil. This difference corresponded to the difference in the amount of Evans blue leakage. The few leaky sites in inflamed ears of K14-Ang1/VEGF mice were located in small venules and in capillary-like vessels, similar to the location of leaky vessels in K14-VEGF mice.
17. I. Baumgartner *et al.*, *Circulation* **97**, 1114 (1998).
18. D. W. Losordo *et al.*, *Circulation* **98**, 2800 (1998).
19. R. M. Schainfeld and J. M. Isner, *Ann. Intern. Med.* **130**, 442 (1999).
20. R. B. Fick Jr. *et al.*, *J. Appl. Physiol.* **63**, 1147 (1987); P. J. Barnes, *J. Allergy Clin. Immunol.* **83**, 1013 (1989); J. S. Erjefalt *et al.*, *Clin. Exp. Allergy* **28**, 1013 (1998); T. Ohrui *et al.*, *J Allergy Clin. Immunol.* **89**, 933 (1992).
21. J. Cunha-Vaz, *Eur. J. Ophthalmol.* **8**, 127 (1998); I. A. Shiels *et al.*, *Med. Hypotheses* **50**, 113 (1998).
22. S. Mesiano, N. Ferrara, R. B. Jaffe, *Am. J. Pathol.* **153**, 1249 (1998).
23. G. Thurston, P. J. Murphy, P. Baluk, J. R. Lindsey, D. M. McDonald, *Am. J. Pathol.* **153**, 1099 (1998).
24. R. K. Bergman and J. J. Munoz, *J. Allergy Clin. Immunol.* **55**, 378 (1975).
25. J. D. Wadsworth, A. Okuno, P. N. Strong, *Biochem. J.* **295**, 537 (1993).
26. G. Thurston, P. Baluk, A. Hirata, D. M. McDonald, *Am. J. Physiol.* **271**, H2547 (1996).
27. P. Baluk, G. Thurston, T. J. Murphy, N. W. Bunnett, D. M. McDonald, *Br. J. Pharmacol.* **126**, 522 (1999).
28. Supported in part by NIH grants HL-59157 and HL-24136. We thank P. Baluk and J. W. McLean for helpful discussions; M. Simmons, T. Murphy, and N. Glazer for technical assistance; and C. Murphy and E. Burrows for help with graphics.

8 July 1999; accepted 8 November 1999

Reduced MAP Kinase Phosphatase-1 Degradation After p42/p44^{MAPK}-Dependent Phosphorylation

Jean-Marc Brondello,* Jacques Pouysségur, Fergus R. McKenzie†

The mitogen-activated protein (MAP) kinase cascade is inactivated at the level of MAP kinase by members of the MAP kinase phosphatase (MKP) family, including MKP-1. MKP-1 was a labile protein in CCL39 hamster fibroblasts; its degradation was attenuated by inhibitors of the ubiquitin-directed proteasome complex. MKP-1 was a target in vivo and in vitro for p42^{MAPK} or p44^{MAPK}, which phosphorylates MKP-1 on two carboxyl-terminal serine residues, Serine 359 and Serine 364. This phosphorylation did not modify MKP-1's intrinsic ability to dephosphorylate p44^{MAPK} but led to stabilization of the protein. These results illustrate the importance of regulated protein degradation in the control of mitogenic signaling.

The control of cell division in response to mitogens is mediated at least in part by MAP kinase (MAPK) signaling pathways (*1*). The p42^{MAPK} and p44^{MAPK} enzymes [extracellular signal–regulated kinase (ERK)–2 and ERK-1] are activated in cells stimulated with mitogens, by phosphorylation on threonine and tyrosine residues within protein kinase subdomain VIII, mediated by a class of MAP kinase (or ERK) kinases typified by MEK1 (*2*). Inhibition of p42^{MAPK} and p44^{MAPK} blocks cell-cycle reentry (*3*) and is principally mediated in vivo by members of a family of dual specificity phosphatases, of which MAP kinase phosphatase (MKP-1, also called 3CH134, CL100, or erp) is archetypal (*4*, *5*). At least nine distinct MKP family members have been cloned, most, if not all, of which are the products of immediate early genes and therefore under tight transcriptional control (*5*, *6*). MKP-1, MKP-2, and MKP-3 are transiently synthesized after activation of p42^{MAPK} and p44^{MAPK}, suggesting the presence of a negative feedback loop to regulate p42^{MAPK} and p44^{MAPK} (*5*–*7*). To determine whether expression of the MKP-1 protein is also subject to control, we determined the half-life of MKP-1 in CCL39 fibroblast cells (Fig. 1A). MKP-1 was barely detectable in quiescent CCL39 fibroblasts, but its expression level was increased in cells stimulated with mitogens before [^{35}S]methionine labeling and immunoprecipitation (*8*). Its half-life was on the order of 45 min.

Because many labile proteins are targeted for degradation by the ubiquitin-directed proteasome complex (*9*), we analyzed the effects of a proteasome inhibitor *N*-acteyl-leu-leu-norleucinal (LLnL) (*10*) and a lysosomal cysteine protease inhibitor, *N*-[*N*-(L-3-trans-carboxiraine-2-carbonyl)-L-leucyl]-agmatine (E64) (*10*) on MKP-1 degradation (Fig. 1B). After treatment of cells with serum to induce synthesis of MKP-1 and blockade of further protein synthesis by cycloheximide, the amount of MKP-1 decreased at a similar rate in control cells and

Institute of Signaling, Developmental Biology and Cancer Research, CNRS UMR 6543, Centre A. Lacassagne, 33 Avenue de Valombrose, Nice 06189, France.

*Present address: The Scripps Research Institute, Department of Molecular Biology, MB-3, 10550 North Torrey Pines Road, La Jolla, CA 92037, USA.

†To whom correspondence should be addressed. E-mail: mckenzie@unice.fr

in the presence of E64, but the rate of degradation of MKP-1 was decreased in the presence of the proteasome inhibitor. Two other proteasome inhibitors Cbz-LLLal (MG132) and Lactacystin (*11*) also attenuated the rate of MKP-1 degradation. MKP-1 was expressed in human embryonic kidney (HEK) 293 cells together with histidine-tagged ubiquitin. The experimental design (*12*, *13*) allows the isolation of multiubiquitinated forms of MKP-1, which are visible as ladders of immunoreactivity on an immunoblot (Fig. 1C).

The inhibition of the proteasome (Fig. 2) was sufficient, on its own, to increase the abundance of MKP-1 and, to a lesser extent, that of MKP-2 in quiescent CCL39 cells (Fig. 2A). After treatment of cells with LLnL, the addition of serum promoted a reduction in MKP-1 mobility in SDS–polyacrylamide gel electrophoresis (SDS-PAGE) (Fig. 2B). To test whether the reduction in MKP-1 mobility was a consequence of phosphorylation, we treated cell extracts containing MKP-1 with phosphatase lambda, which led to the elimination of the more slowly migrating form of MKP-1 (Fig. 2C). Thus, MKP-1 is phosphorylated in response to serum. Examination of MKP-1 primary structure revealed several consensus phosphorylation sites for $p42^{MAPK}$ or $p44^{MAPK}$. To assess whether MKP-1 was phosphorylated by $p42^{MAPK}$ or $p44^{MAPK}$ in vivo, we used CCL39 cells expressing a Raf:estrogen receptor (ER) chimera (*14*), which allows conditional activation of Raf after treatment of the cells with estradiol and concomitant activation of $p45^{MEK1}$, $p42^{MAPK}$, and $p44^{MAPK}$. Treatment of ΔRaf-1::ER-expressing cells labeled with inorganic phosphate with LLnL increased the abundance of MKP-1. When these cells were treated with estradiol, phosphorylation of MKP-1 was increased (Fig. 2D). The inclusion of the $p45^{MEK1}$ inhibitor PD098059 blocked this phosphorylation, indicating that MKP-1 is phosphorylated in an $p45^{MEK1}$-dependent manner.

Purified, active $p44^{MAPK}$ phosphorylated MKP-1 in vitro (*15*, *16*) (Fig. 3A). This phosphorylation was rapid and reversible after addition of phosphatase lambda (*17*). Purified $p45^{MEK1}$ did not phosphorylate MKP-1 under similar conditions but did phosphorylate catalytically inactive $p44^{MAPK}$ (*15*). Although in vitro–translated MKP-1 dephosphorylated $p42^{MAPK}$ and $p44^{MAPK}$, no dephosphorylation of MKP-1 itself was detected (*18*). Taken together, our data indicate that MKP-1 is a substrate for $p42^{MAPK}$ or $p44^{MAPK}$. To identify the site or sites of $p44^{MAPK}$-mediated MKP-1 phosphorylation, we constructed an MKP-1 truncation mutant, MKP-1(1-340), lacking the last 27 COOH-terminal amino acids (*19*) (Fig. 3B). This mutant did not undergo phosphorylation by $p44^{MAPK}$. The $p42^{MAPK}$ and $p44^{MAPK}$ enzymes phosphorylate substrates containing PX(S/T)P (P, proline; X, any neutral or basic

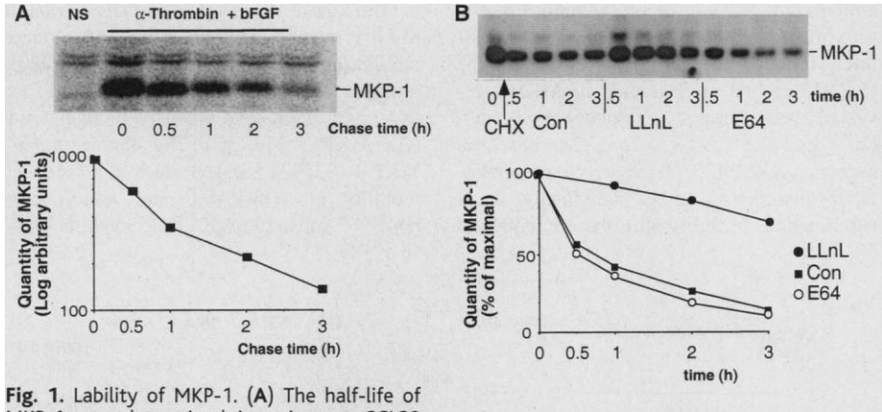

Fig. 1. Lability of MKP-1. (**A**) The half-life of MKP-1 was determined in quiescent CCL39 cells after cell treatment with mitogen [thrombin (1 U/ml) + bovine fibroblast growth factor (bFGF) (10 ng/ml)] for 3 hours, ^{35}S-methionine labeling for 30 min, and addition of unlabeled methionine (1 μM). MKP-1 was immunoprecipitated at the times indicated (chase; h, hours) (*8*), resolved on SDS-PAGE (8.5% gel), and revealed by autoradiography. The bottom panel shows quantitation of immunoprecipitated ^{35}S-labeled MKP-1 by band excision and counting in a scintillation counter. NS, no stimulation. (**B**) Expression of MKP-1 was increased in quiescent CCL39 cells by fetal bovine serum (FBS) (10%, 3 hours) before addition of cycloheximide (CHX, 10 μg/ml) and either LLnL (50 μM), E64 (10 μM), or vehicle (Con). At the times indicated, cells were lysed in a solution of 1% SDS and 4 M urea, and proteins were immunoblotted to reveal MKP-1 (*7*). The bottom panel shows quantitation of MKP-1 in the protein immunoblot by densitometric scanning (MKP-1 at time 0 is 100%). (**C**) Ubiquitination of MKP-1 in vivo. HEK 293 cells were transfected with expression plasmids encoding His-ubiquitin (His-Ub) and MKP-1 (*7*, *12*). After 30 hours, cells were rinsed with ice-cold PBS, and His-ubiquitin conjugates were purified (*12*, *13*). MKP-1 (left) and ubiquitin (right) were detected by protein immunoblotting with antibody to MKP-1 or antisera to ubiquitin, respectively (*7*). The position of MKP-1–ubiquitin conjugates is indicated on the right of each immunoblot.

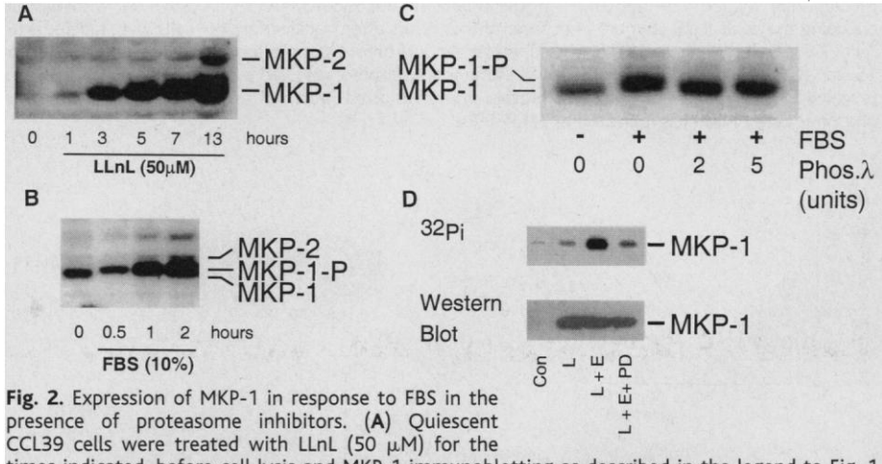

Fig. 2. Expression of MKP-1 in response to FBS in the presence of proteasome inhibitors. (**A**) Quiescent CCL39 cells were treated with LLnL (50 μM) for the times indicated, before cell lysis and MKP-1 immunoblotting as described in the legend to Fig. 1. (**B**) Quiescent CCL39 cells were treated with LLnL (50 μM) for 2 hours, before being stimulated with FBS (10%) for the times indicated; cells were lysed, and MKP-1 was detected by immunoblotting (*7*, *8*). The presence of a more slowly migrating MKP-1 species is indicated by the letter P and is visible 0.5 hours after FBS addition. At 2 hours, MKP-2 is detectable as a poorly resolved band migrating more slowly than MKP-1–P. An additional slowly migrating band is unidentified. (**C**) MKP-1 is phosphorylated in vivo: ΔRaf-1::ER chimera–expressing cells (*14*) were treated with LLnL (50 μM) for 4 hours before FBS stimulation (10%, 10 min), cell lysis, and phosphatase λ (Phos.λ) treatment (*17*). MKP-1 was detected by immunoblotting (*7*, *8*). (**D**) ΔRaf-1::ER chimera–expressing cells were incubated with ^{32}Pi (500 μCi/ml) in phosphate-free medium and left untreated (Con) or treated with LLnL (L, 50 μM) for 4 hours. Cells were stimulated with estradiol (E, 10 μM) with or without PD098059 (PD, 30 μM). Cell lysates were subdivided and MKP-1 was immunoprecipitated, resolved on SDS-PAGE (11% gel), and revealed by autoradiography (top) or protein immunoblotting (bottom) (*7*).

amino acid; S/T, serine or threonine) motifs (*20*). However the first proline is not absolutely required (*21*). Analysis of the last 27 COOH-terminal amino acids of MKP-1 revealed two possible phosphorylation sites, Ser^{359} and Ser^{365}, which are in the consensus sequence XXSP (*22*). Each serine was mutated to alanine (A), either individually or in combination. Mobility shift experiments and in vitro kinase assays revealed that each single MKP-1 mutant exhibited a slightly reduced mobility in SDS-PAGE (Fig. 3C). Both single mutants were also phosphorylated by $p44^{MAPK}$, albeit less extensively than wild-type MKP-1 (Fig. 3C). The double mutant, MKP-1 (S359A, S364A), showed no reduced mobility in SDS-PAGE and was a poor $p44^{MAPK}$ substrate. MKP-1 (S359A, S364A) expressed in HEK293 cells was not phosphorylated after activation of the $p42^{MAPK}$ or $p44^{MAPK}$ cascade in vivo (Fig. 3D). Hence, the major sites of $p44^{MAPK}$-mediated MKP-1 phosphorylation are serines 359 and 364.

Because phosphatases undergo a phosphorylation-dependent modulation of activity (*23*), we sought to determine whether $p42^{MAPK}$- or $p44^{MAPK}$-mediated phosphorylation of MKP-1 modified its activity (Fig. 4). We increased expression of MKP-1 by treating ΔRaf-1::ER-expressing cells with LLnL. After addition of estradiol, the ability of phosphorylated MKP-1 to hydrolyze para-nitrophenylphosphate (p-NPP) (Fig. 4A) and to inactivate $p44^{MAPK}$ was determined (Fig. 4B). Phosphorylated and nonphosphorylated MKP-1 had equal activity to hydrolyze p-NPP and dephosphorylate $p44^{MAPK}$. Thus, it appears that the phosphorylation of MKP-1 by $p42^{MAPK}$ or $p44^{MAPK}$ does not appreciably modify the phosphatase activity of MKP-1.

The transcription factors c-Fos and c-Jun, which are both subject to ubiquitin-directed proteasome degradation, are stabilized as a direct result of MAP kinase–mediated phosphorylation (*24*). To investigate whether $p44^{MAPK}$-mediated phosphorylation of MKP-1 modified its stability, we increased expression of MKP-1 by treating ΔRaf-1::ER-expressing cells with a submaximal concentration of LLnL, which can be removed by repeated washing. After addition of cycloheximide to block further protein synthesis, cells were left untreated or were treated with estradiol to activate $p42^{MAPK}$ or $p44^{MAPK}$ and phosphorylate MKP-1 (Fig. 5).

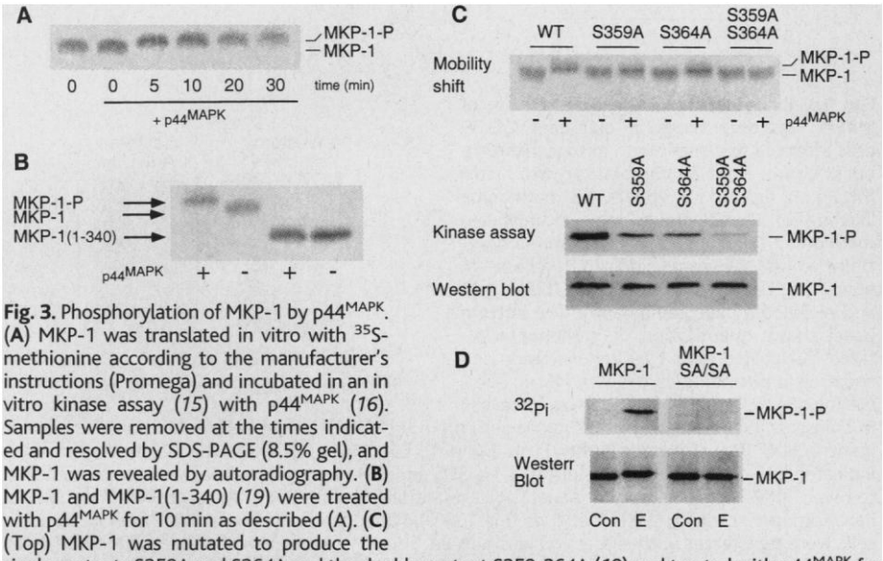

Fig. 3. Phosphorylation of MKP-1 by $p44^{MAPK}$. (**A**) MKP-1 was translated in vitro with ^{35}S-methionine according to the manufacturer's instructions (Promega) and incubated in an in vitro kinase assay (*15*) with $p44^{MAPK}$ (*16*). Samples were removed at the times indicated and resolved by SDS-PAGE (8.5% gel), and MKP-1 was revealed by autoradiography. (**B**) MKP-1 and MKP-1(1-340) (*19*) were treated with $p44^{MAPK}$ for 10 min as described (A). (**C**) (Top) MKP-1 was mutated to produce the single mutants S359A and S364A and the double mutant S359-364A (*19*) and treated with $p44^{MAPK}$ for 10 min as described (A). (Bottom) Wild-type (WT) MKP-1 and the above-mentioned mutants were translated in vitro with unlabeled methionine, subjected to an in vitro kinase assay with $p44^{MAPK}$ and [γ^{32}P]ATP (50 μM, 2 μCi per sample), immunoprecipitated, and detected by protein immunoblotting and autoradiography. (**D**) HEK 293 cells were transiently transfected with expression plasmids encoding Myc-epitope–tagged wild-type MKP-1 or the double mutant S359-364A (SA/SA), together with plasmid encoding the ΔRaf-1::ER chimera (*14*). Twenty-four hours after transfection, the cells were labeled with ^{32}Pi (500 μCi/ml) in phosphate-free medium for 4 hours before stimulation with estradiol (E, 1 μM) for 15 min (Con, no stimulation). MKP-1 was immunoprecipitated, resolved on SDS-PAGE (8.5% gel), and revealed by autoradiography (top) or protein immunoblotted (bottom) as described (*7*). In all cases, phosphorylated MKP-1 is indicated as MKP-1–P.

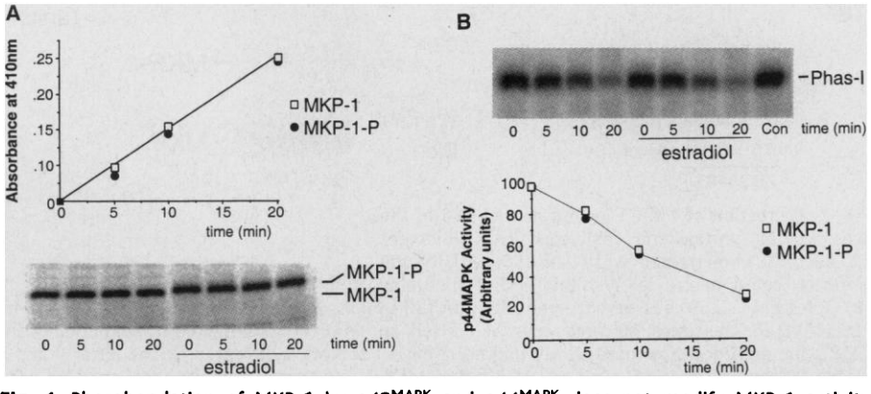

Fig. 4. Phosphorylation of MKP-1 by $p42^{MAPK}$ and $p44^{MAPK}$ does not modify MKP-1 activity. ΔRaf-1::ER chimera–expressing cells were treated with LLnL (50 μM) for 4 hours. Cells were then left untreated or treated with estradiol (1μM, 15 min), and MKP-1 was immunoprecipitated. (**A**) (Top) The ability of nonphosphorylated (MKP-1) or $p42^{MAPK}$- or $p44^{MAPK}$-phosphorylated MKP-1 (MKP-1–P) to hydrolyze p-NPP was determined at the times indicated (*18*). (Bottom) Immunoprecipitated MKP-1 and MKP-1–P were subjected to protein immunoblotting. (**B**) $p44^{MAPK}$ was in vitro dephosphorylated by immunoprecipitated MKP-1 or MKP-1–P [produced as in (A)] (*7*, *26*), and remaining $p44^{MAPK}$ activity was determined by an in vitro kinase assay with PHAS-I as substrate (*15*) (top). The bottom panel shows the quantification of the data by densitometric scanning.

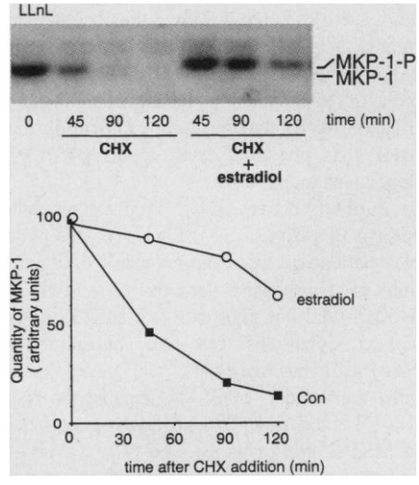

Fig. 5. MKP-1 is stabilized by activation of the $p42^{MAPK}$ and $p44^{MAPK}$ cascade. ΔRaf-1::ER chimera–expressing cells were treated with LLnL (10 μM) for 2 hours, before extensive cell washing to remove LLnL. Cells were treated with cycloheximide (CHX, 10 μg/ml) or CHX with estradiol (1 μM). Cells were lysed at the times indicated, and MKP-1 was detected by protein immunoblotting (**top**) followed by densitometric quantitation (**bottom**).

The degradation rate of MKP-1 after activation of $p42^{MAPK}$ or $p44^{MAPK}$ was less than half that in the absence of estradiol. Under the same conditions, the degradation rate of inhibitor of κBα (IκBα) in response to tumor necrosis factor–α was unaltered in ΔRaf-1::ER-expressing cells after addition of estradiol (*18*). Hence, phosphorylation of MKP-1 by $p42^{MAPK}$ or $p44^{MAPK}$ serves to reduce ubiquitin-dependent degradation of the phosphatase. Activation of $p42^{MAPK}$ or $p44^{MAPK}$ therefore regulates MKP-1 protein expression through both an up-regulation of the rate of transcription (*7*) and a reduction in the rate of proteasome-mediated degradation.

The $p42^{MAPK}$ and $p44^{MAPK}$ enzymes have a central role in the capacity of cells to divide in response to growth factors. Activation of $p42^{MAPK}$ and $p44^{MAPK}$ is a prerequisite for cell-cycle reentry (*3*). However, inappropriate or constitutive activation of the $p42^{MAPK}$ or $p44^{MAPK}$ cascade may provoke cellular senescence (*25*). Taken together, these findings illustrate a complex control mechanism designed to limit undesirable long-term activation of $p42^{MAPK}$ and $p44^{MAPK}$ and further demonstrate the importance of regulated protein degradation to the control of cell division processes.

References and Notes

1. M. J. Robinson and M. H. Cobb, *Curr. Opin. Cell Biol.* **9**, 180 (1997); P. Cohen, *Trends. Cell. Biol.* **7**, 353 (1997); T. S. Lewis, P. S. Shapiro, N. G. Ahn, *Adv. Cancer Res.* **74**, 49 (1998).
2. C. M. Crews, A. Alessandrini, R. L. Erikson, *Science* **258**, 478 (1992); R. Seger *et al.*, *J. Biol. Chem.* **267**, 14373 (1992); J. Wu *et al.*, *Mol. Cell. Biol.* **13**, 4539 (1993); C. F. Zheng and K. L. Guan, *J. Biol. Chem.* **268**, 11435 (1993).
3. G. Pages *et al.*, *Proc. Natl. Acad. Sci. U.S.A.* **90**, 8319 (1993); H. Sun, N. K. Tonks, D. Bar-Sagi, *Science* **266**, 285 (1994); J. A. Frost, T. D. Geppert, M. H. Cobb, J. R. Feramisco, *Proc. Natl. Acad. Sci. U.S.A.* **91**, 3844 (1994); J. Troppmair *et al.*, *J. Biol. Chem.* **269**, 7030 (1994); J. M. Brondello, F. R. McKenzie, H. Sun, N. K. Tonks, J. Pouysségur, *Oncogene* **10**, 1895 (1995).
4. S. M. Keyse and E. A. Emslie, *Nature* **359**, 644 (1992); C. H. Charles, A. S. Abler, L. F. Lau, *Oncogene* **7**, 197 (1992); T. Noguchi *et al.*, *Mol. Cell. Biol.* **13**, 5195 (1993).
5. S. M. Keyse, *Semin. Cell Dev. Biol.* **9**, 143 (1998).
6. D. Bokemeyer *et al.*, *J. Biol. Chem.* **271**, 639 (1996); S. J. Cook, J. Beltman, W. A. Cadwallader, M. McMahon, F. McCormick, *J. Biol. Chem.* **272**, 13309 (1997); J. C. Scimeca, M. J. Servant, J. O. Dyer, S. Meloche, *Oncogene* **15**, 717 (1997).
7. J. M. Brondello, D. Roux, G. Pages, J. Pouysségur, F. R. McKenzie, unpublished results; J. M. Brondello, J. Pouysségur, F. R. McKenzie, *J. Biol. Chem.* **272**, 1368 (1997).
8. Cell lysis and protein immunoblotting of MKP-1 and -2 were performed exactly as described (*7*). For immunoprecipitation of MKP-1, cells were washed with ice-cold phosphate-buffered saline (PBS) and lysed with Triton X-100 lysis buffer [50 mM tris-HCl (pH 7.5), 100 mM NaCl, 50 mM NaF, 5 mM EDTA, 40 mM β-glycerophosphate, 200 μM sodium orthovanadate, 10^{-4} M phenylmethylsulfonyl fluoride, leupeptin (1 μg/ml), 1 μM peptstatin A, and 1% (v/v) Triton X-100] as described for protein immunoblot analysis. Proteins from lysates (400 μg) were incubated with antibodies to MKP-1 (*7*) preadsorbed to protein A–Sepharose–coated beads for 2 hours at 4°C. Immune complexes were washed three times with Triton X-100 lysis buffer before resolution on SDS-PAGE (9% gels).
9. R. W. King, R. J. Deshaies, J.-M. Peters, M. W. Kirschner, *Science* **274**, 1652 (1996); M. Hochstrasser, *Annu. Rev. Genet.* **30**, 405 (1996).
10. J. Adams and R. Stein, *Annu. Rep. Med. Chem.* **31**, 279 (1996).
11. G. Fenteany *et al.*, *Science* **268**, 726 (1995).
12. M. Treier, L. M. Staszewski, D. Bohmann, *Cell* **78**, 787 (1994).
13. The His6-tagged expression vectors were as described (*12*). Purification of MKP-1–ubiquitin conjugates was performed exactly as described (*12*).
14. P. Lenormand, M. McMahon, J. Pouysségur, *J. Biol. Chem.* **271**, 15762 (1996).
15. In vitro kinase assays were performed in 50 mM Hepes (pH 7.5), 20 mM $MgCl_2$, 1 mM dithiothreitol, and 10 mM p-NPP with either 500 μM adenosine triphosphate (ATP) or 50 μM ATP and [^{32}Pγ]ATP [2 μCi per sample together with 1 ng of active $p44^{MAPK}$ (*16*) or $GSTp45^{MEK}$ (S/D, S/D; D, Asp), which was purified in *Escherichia coli* as a GST fusion protein and purified by binding to glutathione-Sepharose]. Reactions were terminated by addition of 1% SDS and 4 M urea and resolution of samples on SDS-PAGE (9% gels).
16. A. Khokhtalchev *et al.*, *J. Biol. Chem.* **272**, 11057 (1997).
17. CCL39 cells (2.5×10^6 cells per well, six-well plate) were lysed in Triton X-100 lysis buffer [50 mM tris-HCl (pH 7.5), 100 mM NaCl, 50 mM NaF, 5 mM EDTA, 10^{-4} M phenylmethylsulfonyl fluoride, leupeptin (1 μg/ml), 1 μM pepstatin A, and 1% (v/v) Triton X-100; phosphatase λ was added together with $MnCl_2$ (1 mM final)]. After 15 min, reactions were stopped by addition of 1% SDS and 4 M urea, and samples (50 μg of protein) were resolved on SDS-PAGE (9% gel) and immunoblotted to detect MKP-1 (*7*).
18. J.-M. Brondello and F. R. McKenzie, unpublished results; K. Guan, S. S. Broyles, J. E. Dixon, *Nature* **350**, 359 (1991). Immunoprecipitated MKP-1 phosphatase activity was measured in 200 μl of solution containing 10 mM Imidazole (pH 7.5), 0.1% β-mercaptoethanol, and 10 mM p-NPP at 30°C for the times indicated. The reaction was stopped by addition of 500 μl of 0.25 M NaOH. Absorbance at 410 nm was measured. Nonspecific p-NPP hydrolysis in immunoprecipitates of cells transfected with vector was subtracted from the data.
19. MKP-1 underwent polymerase chain reaction–directed mutagenesis with the following primers: ATG primer, 5′-GCCAGCCATGGTCATGGAAGTG-3′; S364A primer, 5′-GCAGCTGGGAGCGGTCGTAATGGGGCTCTGAAGGTAGC-3′; S359A primer, 5′-GCAGCTGGGAGAGGTCGTAATGGGGGCCTGAAGGTAGC-3′; S359/364A primer, 5′-GCAGCTGGGAGCGGTCGTAATGGGGGCCTGAAGGTAGC-3′; and truncation at amino acid 340 primer, 5′-GTTGAACACGGTGGTGGTGGA-3′. After amplification, DNA was subcloned into pCRII followed by pcDNA3.1(+) in frame with a Myc-epitope tag. All mutations were verified by sequencing.
20. I. Clark-Lewis, J. S. Sanghera, S. L. Pelech, *J. Biol. Chem.* **266**, 15180 (1991); F. A. Gonzalez, D. L. Raden, R. J. Davis, *J. Biol. Chem.* **266**, 22159 (1991).
21. J. W. Haycock, N. G. Ahn, M. H. Cobb, E. G. Krebs, *Proc. Natl. Acad. Sci. U.S.A.* **89**, 2365 (1992); S. Corbalan-Garcia, S.-S. Yang, K. R. Degenhardt, D. Bar-Sagi, *Mol. Cell. Biol.* **16**, 5674 (1996).
22. Serines 359 and 364 within the consensus sequence XXSP, where X represents a neutral or basic amino acid, are present in MKP-1 (mouse and human sequences) and MKP-2 (human and rat sequences). MKP-1 and -2 share 62% overall sequence identity.
23. N. Rivard, F. R. McKenzie, J.-M. Brondello, J. Pouysségur, *J. Biol. Chem.* **270**, 11017 (1995); B. G. Neel and N. K. Tonks, *Curr. Opin. Cell Biol.* **9**, 193 (1997).
24. K. Okazaki and N. Sagata, *EMBO J.* **14**, 5048 (1995); A. M. Musti, M. Treier, D. Bohmann, *Science* **275**, 400 (1997).
25. J. Zhu, D. Woods, M. McMahon, J. M. Bishop, *Genes Dev.* **12**, 2997 (1998); A. W. Lin *et al.*, *Genes Dev.* **12**, 3008 (1998).
26. After MKP-1 immunoprecipitation (*7*), active $p44^{MAPK}$ (10 ng/ml) was added to immunoprecipitates in a final volume of 100 μl containing 50 mM Hepes (pH 7.0), 60 mM NaCl, 60 mM KCl, bovine serum albumin (1 mg/ml), and 5 mM EGTA. Reactions proceeded at 30°C for the times indicated and terminated by addition of 200 μM sodium orthovanadate. A kinase assay to determine $p44^{MAPK}$ activity was then performed (*15*) with PHAS-I as substrate.

27. We thank D. Bohmann for His-ubiquitin expression plasmid, all members of the Pouysségur laboratory for their support, and K. Marcu for financial assistance. Supported by the CNRS, the Institut National de la Sante et de la Recherche Medicale, the Association pour la Recherche contre le Cancer, and NIH grant GM26939 awarded to K. Marcu. B.J.M. was supported by the Ligue Nationale contre le Cancer.

19 May 1999; accepted 22 November 1999

Bacteriophytochromes: Phytochrome-Like Photoreceptors from Nonphotosynthetic Eubacteria

Seth J. Davis,[1] Alexander V. Vener,[2] Richard D. Vierstra[1,2]*

Phytochromes are a family of photoreceptors used by green plants to entrain their development to the light environment. The distribution of these chromoproteins has been expanded beyond photoautotrophs with the discovery of phytochrome-like proteins in the nonphotosynthetic eubacteria *Deinococcus radiodurans* and *Pseudomonas aeruginosa*. Like plant phytochromes, the *D. radiodurans* receptor covalently binds linear tetrapyrroles autocatalytically to generate a photochromic holoprotein. However, the attachment site is distinct, using a histidine to potentially form a Schiff base linkage. Sequence homology and mutational analysis suggest that *D. radiodurans* bacteriophytochrome functions as a light-regulated histidine kinase, which helps protect the bacterium from visible light.

The phytochrome family of dimeric photoreceptors regulates growth and development by sensing ambient light through the photointerconversion between an inactive red-light (R)–absorbing form and an active far-red-light (FR)–absorbing form (*1*). Although previously thought to be restricted to higher plants, the recent detection of phytochrome-like proteins

References and Notes

[2] **The Primary Structure of MEK, a Protein Kinase That Phosphorylates the ERK Gene Product**

Craig M. Crews; Alessandro Alessandrini; Raymond L. Erikson

Science, New Series, Vol. 258, No. 5081. (Oct. 16, 1992), pp. 478-480.

Stable URL:

http://links.jstor.org/sici?sici=0036-8075%2819921016%293%3A258%3A5081%3C478%3ATPSOMA%3E2.0.CO%3B2-2

[3] **Mitogen-Activated Protein Kinases p42 ^{mapk} and p44 ^{mapk} are Required for Fibroblast Proliferation**

Gille Pages; Philippe Lenormand; Gilles L'Allemain; Jean-Claude Chambard; Sylvain Meloche; Jacques Pouyssegur

Proceedings of the National Academy of Sciences of the United States of America, Vol. 90, No. 18. (Sep. 15, 1993), pp. 8319-8323.

Stable URL:

http://links.jstor.org/sici?sici=0027-8424%2819930915%2990%3A18%3C8319%3AMPKPAP%3E2.0.CO%3B2-R

[3] **Inhibition of Ras-Induced DNA Synthesis by Expression of the Phosphatase MKP-1**

Hong Sun; Nicholas K. Tonks; Dafna Bar-Sagi

Science, New Series, Vol. 266, No. 5183. (Oct. 14, 1994), pp. 285-288.

Stable URL:

http://links.jstor.org/sici?sici=0036-8075%2819941014%293%3A266%3A5183%3C285%3AIORDSB%3E2.0.CO%3B2-8

LINKED CITATIONS

[3] **A Requirement for Extracellular Signal-Regulated Kinase (ERK) Function in the Activation of AP-1 by Ha-Ras, Phorbol 12-Myristate 13-Acetate, and Serum**

Jeffrey A. Frost; Thomas D. Geppert; Melanie H. Cobb; James R. Feramisco

Proceedings of the National Academy of Sciences of the United States of America, Vol. 91, No. 9. (Apr. 26, 1994), pp. 3844-3848.

Stable URL:

http://links.jstor.org/sici?sici=0027-8424%2819940426%2991%3A9%3C3844%3AARFESK%3E2.0.CO%3B2-K

[9] **How Proteolysis Drives the Cell Cycle**

Randall W. King; Raymond J. Deshaies; Jan-Michael Peters; Marc W. Kirschner

Science, New Series, Vol. 274, No. 5293. (Dec. 6, 1996), pp. 1652-1659.

Stable URL:

http://links.jstor.org/sici?sici=0036-8075%2819961206%293%3A274%3A5293%3C1652%3AHPDTCC%3E2.0.CO%3B2-D

[11] **Inhibition of Proteasome Activities and Subunit-Specific Amino-Terminal Threonine Modification by Lactacystin**

Gabriel Fenteany; Robert F. Standaert; William S. Lane; Soongyu Choi; E. J. Corey; Stuart L. Schreiber

Science, New Series, Vol. 268, No. 5211. (May 5, 1995), pp. 726-731.

Stable URL:

http://links.jstor.org/sici?sici=0036-8075%2819950505%293%3A268%3A5211%3C726%3AIOPAAS%3E2.0.CO%3B2-W

[21] **ERK1 and ERK2, Two Microtubule-Associated Protein 2 Kinases, Mediate the Phosphorylation of Tyrosine Hydroxylase at Serine-31 In situ**

John W. Haycock; Natalie G. Ahn; Melanie H. Cobb; Edwin G. Krebs

Proceedings of the National Academy of Sciences of the United States of America, Vol. 89, No. 6. (Mar. 15, 1992), pp. 2365-2369.

Stable URL:

http://links.jstor.org/sici?sici=0027-8424%2819920315%2989%3A6%3C2365%3AEAETMP%3E2.0.CO%3B2-8

[24] **Reduced Ubiquitin-Dependent Degradation of c-Jun After Phosphorylation by MAP Kinases**

Anna Maria Musti; Mathias Treier; Dirk Bohmann

Science, New Series, Vol. 275, No. 5298. (Jan. 17, 1997), pp. 400-402.

Stable URL:

http://links.jstor.org/sici?sici=0036-8075%2819970117%293%3A275%3A5298%3C400%3ARUDOCA%3E2.0.CO%3B2-I